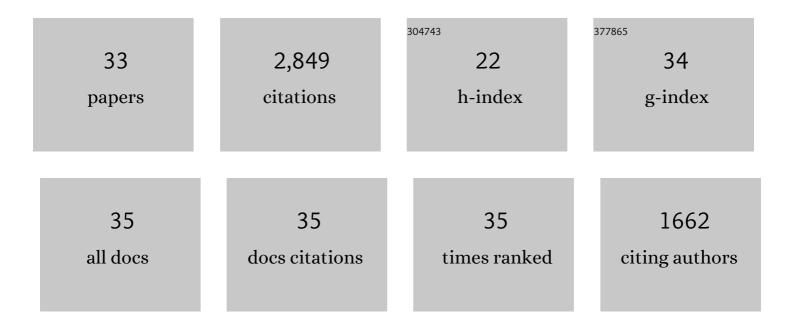
Artur Deditius

List of Publications by Year in descending order

Source: https://exaly.com/author-pdf/1725508/publications.pdf Version: 2024-02-01



#	Article	IF	CITATIONS
1	The coupled geochemistry of Au and As in pyrite from hydrothermal ore deposits. Geochimica Et Cosmochimica Acta, 2014, 140, 644-670.	3.9	400
2	Pyrite as a record of hydrothermal fluid evolution in a porphyry copper system: A SIMS/EMPA trace element study. Geochimica Et Cosmochimica Acta, 2013, 104, 42-62.	3.9	335
3	Trace metal nanoparticles in pyrite. Ore Geology Reviews, 2011, 42, 32-46.	2.7	327
4	A proposed new type of arsenian pyrite: Composition, nanostructure and geological significance. Geochimica Et Cosmochimica Acta, 2008, 72, 2919-2933.	3.9	278
5	Trace elements in magnetite from massive iron oxide-apatite deposits indicate a combined formation by igneous and magmatic-hydrothermal processes. Geochimica Et Cosmochimica Acta, 2015, 171, 15-38.	3.9	203
6	Giant Kiruna-type deposits form by efficient flotation of magmatic magnetite suspensions. Geology, 2015, 43, 591-594.	4.4	177
7	Geochemical and micro-textural fingerprints of boiling in pyrite. Geochimica Et Cosmochimica Acta, 2019, 246, 60-85.	3.9	137
8	TRACE ELEMENT SIGNATURE OF PYRITE FROM THE LOS COLORADOS IRON OXIDE-APATITE (IOA) DEPOSIT, CHILE: A MISSING LINK BETWEEN ANDEAN IOA AND IRON OXIDE COPPER-GOLD SYSTEMS?. Economic Geology, 2016, 111, 743-761.	3.8	120
9	Decoupled geochemical behavior of As and Cu in hydrothermal systems. Geology, 2009, 37, 707-710.	4.4	108
10	Copper–arsenic decoupling in an active geothermal system: A link between pyrite and fluid composition. Geochimica Et Cosmochimica Acta, 2017, 204, 179-204.	3.9	93
11	The role of bacterial sulfate reduction during dolomite precipitation: Implications from Upper Jurassic platform carbonates. Chemical Geology, 2015, 412, 1-14.	3.3	79
12	"Invisible―silver and gold in supergene digenite (Cu1.8S). Geochimica Et Cosmochimica Acta, 2010, 74, 6157-6173.	3.9	66
13	The chemical stability of coffinite, USiO4·nH2O; 0 <n<2, 2008,="" 251,="" 33-49.<="" a="" associated="" case="" chemical="" from="" geology,="" grants="" matter:="" mexico,="" new="" organic="" region,="" study="" td="" uranium="" usa.="" with=""><td>3.3</td><td>64</td></n<2,>	3.3	64
14	Nanoscale "liquid" inclusions of As-Fe-S in arsenian pyrite. American Mineralogist, 2009, 94, 391-394.	1.9	53
15	Synthesis and characterization of coffinite. Journal of Nuclear Materials, 2009, 393, 449-458.	2.7	46
16	Constraints on the solid solubility of Hg, Tl, and Cd in arsenian pyrite. American Mineralogist, 2016, 101, 1451-1459.	1.9	46
17	New contributions to the understanding of Kiruna-type iron oxide-apatite deposits revealed by magnetite ore and gangue mineral geochemistry at the El Romeral deposit, Chile. Ore Geology Reviews, 2018, 93, 413-435.	2.7	43
18	Super-sieving effect in phenol adsorption from aqueous solutions on nanoporous carbon beads. Carbon, 2018, 135, 12-20.	10.3	34

ARTUR DEDITIUS

#	Article	IF	CITATIONS
19	Fate of trace elements during alteration of uraninite in a hydrothermal vein-type U-deposit from Marshall Pass, Colorado, USA. Geochimica Et Cosmochimica Acta, 2007, 71, 4954-4973.	3.9	30
20	Nanogeoscience in ore systems research: Principles, methods, and applications. Ore Geology Reviews, 2011, 42, 1-5.	2.7	28
21	A genetic link between magnetite mineralization and diorite intrusion at the El Romeral iron oxide-apatite deposit, northern Chile. Mineralium Deposita, 2018, 53, 947-966.	4.1	26
22	lodine-rich waters involved in supergene enrichment of the Mantos de la Luna argentiferous copper deposit, Atacama Desert, Chile. Mineralium Deposita, 2009, 44, 719-722.	4.1	20
23	Crystal chemistry and radiation-induced amorphization of P-coffinite from the natural fission reactor at Bangombe, Gabon. American Mineralogist, 2009, 94, 827-837.	1.9	18
24	Dissecting the Re-Os molybdenite geochronometer. Scientific Reports, 2017, 7, 16054.	3.3	15
25	Role of vein-phases in nanoscale sequestration of U, Nb, Ti, and Pb during the alteration of pyrochlore. Geochimica Et Cosmochimica Acta, 2015, 150, 226-252.	3.9	14
26	Nanoscale partitioning of Ru, Ir, and Pt in base-metal sulfides from the Caridad chromite deposit, Cuba. American Mineralogist, 2018, 103, 1208-1220.	1.9	14
27	Formation of nanoscale Th-coffinite. American Mineralogist, 2012, 97, 681-693.	1.9	12
28	Precipitation and alteration of coffinite (USiO4nH2O) in the presence of apatite. European Journal of Mineralogy, 2010, 22, 75-88.	1.3	10
29	Leaching of brannerite in the ferric sulphate system. Part 2: Mineralogical transformations during leaching. Hydrometallurgy, 2016, 159, 95-106.	4.3	9
30	Constraints on Hf and Zr mobility in high-sulfidation epithermal systems: formation of kosnarite, KZr2(PO4)3, in the Chaquicocha gold deposit, Yanacocha district, Peru. Mineralium Deposita, 2015, 50, 429-436.	4.1	3
31	Arsenic-Environmental Geochemistry, Mineralogy, and Microbiology. Reviews in Mineralogy and Geochemistry, Volume 79 (R.J. Bowell, C.N. Alpers, H.E. Jamieson, D.K. Nordstron, and J. Majzlan, eds.). Economic Geology, 2015, 110, 1905-1907.	3.8	3
32	Phenol Molecular Sheets Woven by Water Cavities in Hydrophobic Slit Nanospaces. Langmuir, 2018, 34, 15150-15159.	3.5	1
33	Microbeam Analysis of Plasma Effects in Synthetic Mica-Like Compound. Microscopy and Microanalysis, 2008, 14, 1426-1427.	0.4	0